Superconductivity at 2.5 K in new transition-metal chalcogenide Ta_2PdSe_5

J. Zhang[1], J. K. Dong[1,2(a)], Y. Xu[1], J. Pan[1], L. P. He[1], L. J. Zhang[2], and S. Y. Li[1,2,3(b)]

[1]*State Key Laboratory of Surface Physics and Department of Physics, Fudan University, Shanghai 200433, P. R. China*
[2]*Laboratory of Advanced Materials, Fudan University, Shanghai 200438, P. R. China*
[3]*Collaborative Innovation Center of Advanced Microstructures, Fudan University, Shanghai 200433, P. R. China*

arXiv:1412.6983v3 [cond-mat.supr-con] 13 Apr 2015

PACS 74.70.Xa – Pnictides and chalcogenides
PACS 74.25.Bt – Thermodynamic properties
PACS 74.25.F- – Transport properties

Abstract –We report the synthesis and superconducting properties of a new transition-metal chalcogenide Ta_2PdSe_5. The measurements of resistivity, magnetization, and specific heat reveal that Ta_2PdSe_5 is a bulk superconductor with $T_c \simeq 2.5$ K. The zero-field electronic specific heat in the superconducting state can be fitted with a two-gap BCS model. The upper critical field H_{c2} shows a linear temperature dependence, and the value of $H_{c2}(0)$ is much higher than the estimated Pauli limiting field H_{c2}^P and orbital limiting field H_{c2}^{orb}. All these results of specific heat and upper critical field suggest that Ta_2PdSe_5 is a multi-band superconductor.

Introduction. – For BCS superconductors with spin-singlet pairing, magnetic field destroys the superconductivity by either orbital effect or Pauli paramagnetic effect. The upper critical field H_{c2} which reflects the pair-breaking mechanism is usually limited by the orbital effect, with the limiting field $H_{c2}^{orb} = \Phi_0/2\pi\xi^2$. Pauli paramagnetic effect becomes important when the orbital contribution is somehow suppressed or when the normal-state spin susceptibility χ_N is enhanced due to spin-orbit coupling, resulting in the Pauli limiting field H_{c2}^P smaller than H_{c2}^{orb} [1]. Then the spin polarization determines the upper critical field $H_{c2}^P = 1.84\,T_c$, within the weak-coupling BCS theory [2]. Experimentally, superconductivity with H_{c2} beyond H_{c2}^P has been observed in some low-dimensional materials, such as the organic Bechgaard salt $(TMTSF)_2PF_6$ [3], purple bronze $Li_{0.9}Mo_6O_{17}$ [4], and iron chalcogenide β-FeSe [5]. Different theories including spin-triplet pairing, strong spin-orbit coupling, and multi-band effect are proposed [3–5]. For practical applications, the superconductors with high H_{c2} are more promising in high-field application.

Recently, a new quasi-one-dimentional (Q1D) transition-metal chalcogenide $Nb_2Pd_{0.81}S_5$ was synthesized, in the monoclinic space group $C2/m$ [6]. It becomes a superconductor below the transition temperature $T_c \simeq 6.6$ K [6]. Later, the two existing compounds Ta_2PdS_5 and Nb_2PdSe_5 with the same crystal structure [7], were also found to be superconducting below 6 K and 5.5 K, respectively [8, 9]. All these three compounds display extremely high and anisotropic H_{c2} [6, 8–11], suggesting a new family of exotic superconductors T_2PdCh_5 (T = Nb or Ta, Ch = S or Se).

Unconventional spin-triplet pairing state has been discussed based on the quasi-one dimensionality of T_2PdCh_5, which may explain the unusual H_{c2} [6,8,9]. However, this proposal is challenged by the robustness of the H_{c2}/T_c ratio in the Se substitution experiment in Nb_2PdS_5 [12]. The spin-orbit coupling was also considered as one possible origin of the high H_{c2} in this family [8, 9]. This proposal is supported by the opposite substituting effect on the H_{c2}/T_c ratio in Nb_2PdS_5 [13]. The substitution of Pd by heavier Pt enhances the H_{c2}/T_c ratio, while lighter Ni substitution decreases it [13]. Alternatively, multi-band effect could also give rise to their high H_{c2} values [6, 8, 12, 13]. Electronic structure calculations have shown that all these three compounds are multi-band superconductors with several sheets of Fermi surface [6,8,14]. Since the origin of the enhanced H_{c2} is still not clear, finding more compounds in this family may provide us better un-

(a)E-mail: jkdong@fudan.edu.cn
(b)E-mail: shiyan_li@fudan.edu.cn

derstanding of their unusual H_{c2}/T_c.

In this letter, we report the synthesis and superconducting properties of a new transition-metal chalcogenide Ta_2PdSe_5, the fourth member of T_2PdCh_5 family. Measurements of electrical resistivity, magnetization and specific heat confirm bulk superconductivity in this material, with $T_c \simeq 2.5$ K. Both the fit of electronic specific heat and the linear temperature dependence of $H_{c2}(T)$ support multi-band superconductivity in Ta_2PdSe_5. The ratio of H_{c2}/T_c is as high as 6 T/K, which may also be ascribed to the multi-band effect.

Experimental details. – The polycrystalline samples of Ta_2PdSe_5 were synthesized by a conventional solid state reaction method. The starting materials of Ta(99.99%), Pd(99.99%), and Se(99.99%) powders were mixed thoroughly in the ratio of 2:1:5.5 and pressed into pellets in a argon-filled glove box. Excess amount of Se is necessary to compensate the loss of Se during the reaction due to its high vapor pressure. The pellets were placed in a quartz tube, slowly heated to 750°C at a rate of 10°C/h and then kept at this temperature for 48 hours before shutting down the furnace. This process was repeated four times, and the finally obtained samples are stable in air. X-ray diffraction (XRD) measurement was performed by using an X-ray diffractometer (D8 Advance, Bruker) with Cu $K\alpha$ radiation. The dc magnetization was measured in a Superconducting Quantum Interference Device (SQUID, Quantum Design). Electrical resistivity measurements were performed in ^{4}He and ^{3}He cryostats, by a standard four-probe technique. The low-temperature specific heat was measured from 0.3 to 10 K in a Physical Property Measurement System (PPMS, Quantum Design) equipped with a small dilution refrigerator.

Results and Discussion. – Figure 1 shows the powder X-ray diffraction (XRD) pattern of Ta_2PdSe_5 taken at room temperature. Most of the peaks can be well indexed to a monoclinic structure with space group $C2/m$. The observed XRD pattern is refined by a Rietveld method using TOPAS Academic package, from which Ta_2PdSe_5 is recognized as the main phase, with a small amount of Pd_7Se_4 impurity. The refined lattice parameters of Ta_2PdSe_5 are $a = 12.801(5)$ Å, $b = 3.117(1)$ Å, $c = 17.742(3)$ Å, $\alpha = \gamma = 90°$, and $\beta = 106.22(2)°$. A perspective view of the Ta_2PdSe_5 crystal structure along b-axis direction is shown in the inset of Fig. 1. The one-dimensional Ta-Se chains along the b axis are bridged by $PdSe_4$ squares. This compound is the fourth member of T_2PdCh_5 (T = Nb or Ta, Ch = S or Se) family.

Figure 2(a) plots the low-temperature dc magnetization of Ta_2PdSe_5 in $H = 10$ Oe, with both zero-field-cooled (ZFC) and field-cooled (FC) processes. The diamagnetic signal reveals a superconducting transition with the onset T_c at about 2.6 K. Figure 2(b) shows the temperature dependence of resistivity for Ta_2PdSe_5 measured between 1.5 and 300 K. $\rho(T)$ displays metallic behavior with a residual resistivity ratio RRR = $\rho(294\text{ K})/\rho(3\text{ K}) \simeq 3.3$.

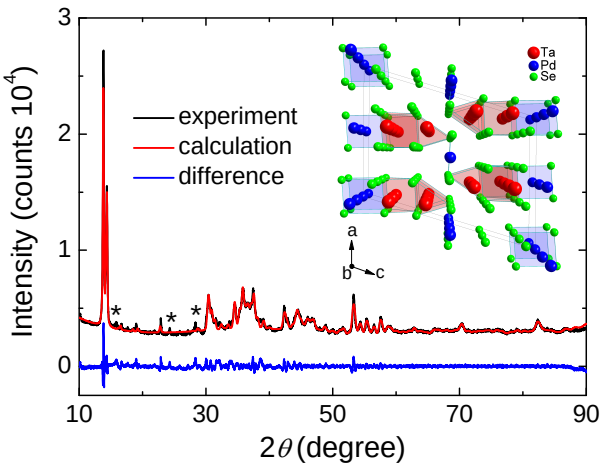

Fig. 1: (Color online) X-ray diffraction pattern of a Ta_2PdSe_5 polycrystalline sample measured at room temperature. The black line corresponds to the experimental XRD data, and the red line is a Rietveld refinement fit with $C2/m$ space group. The blue line is their difference. The refined lattice parameters are $a = 12.801(5)$ Å, $b = 3.117(1)$ Å, $c = 17.742(3)$ Å, $\alpha = \gamma = 90°$, and $\beta = 106.22(2)°$. The asterisks mark the peaks of a small amount of Pd_7Se_4 impurity. The inset shows the crystal structure of Ta_2PdSe_5, an perspective view along the b-axis direction.

The inset shows the resistivity at low temperature ranging from 1 to 5 K. A clear drop of resistivity is observed, corresponding to the superconducting transition. The onset, mid-point and zero-point temperatures of the resistive transition (T_c^{onset}, T_c^{mid} and T_c^{zero}) are 2.5, 2.2, and 2.0 K, respectively. The T_c^{onset} is determined from the intersection of the two extrapolated lines near the transition, as seen in the inset. The T_c^{mid} and T_c^{zero} are defined at the temperatures where the normal-state resistivity drops by half and to zero, respectively. The width of the resistive superconducting transition ΔT_c is about 0.5 K.

Figure 3(a) plots the specific heat divided by the temperature, C_p/T, as a function of temperature in various magnetic fields. C_p/T shows an anomaly around 2.5 K in zero field, corresponding to the superconducting transition. This anomaly shifts to lower temperature and becomes less pronounced with increasing magnetic field, as shown in the inset. Above T_c, the zero-field data can be well fitted by $C_p/T = \gamma + \beta T^2 + \delta T^4$ from 3.5 to 10 K. We determine the electronic specific heat coefficient γ, the phononic coefficients β to be 10.3 mJ mol^{-1} K^{-2} and 3.2 mJ mol^{-1} K^{-4}, respectively. The Debye temperature $\Theta_D \simeq 169$ K is estimated from the equation $\beta = (12\pi^4 n k_B)/(5\Theta_D^3)$, where n is the number of atoms per formula unit.

The zero-field electronic specific heat C_e/T obtained by subtracting the lattice terms from C_p is depicted in Fig. 3(b). The bulk nature of the superconductivity in Ta_2PdSe_5 is confirmed by the significant jump of C_e/T. In order to get more information about the superconduct-

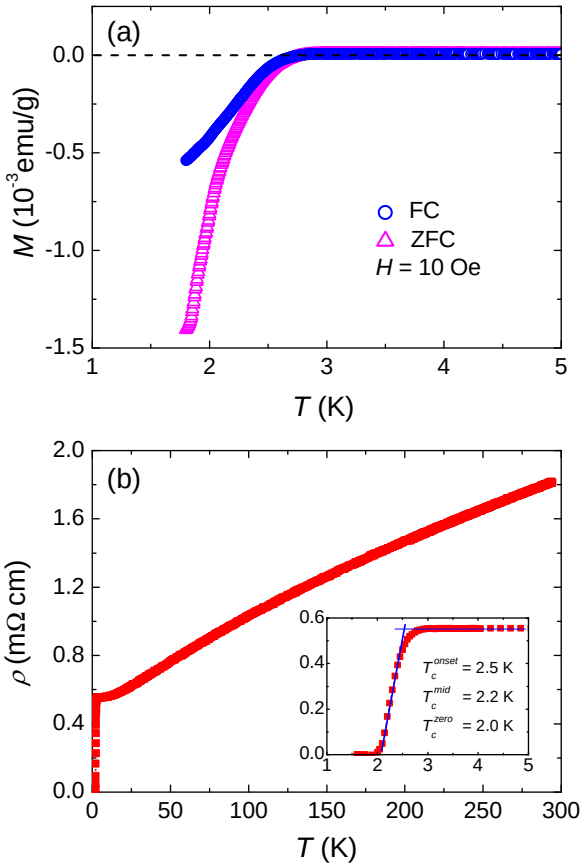

Fig. 2: (Color online) (a) Low-temperature dc magnetization of Ta_2PdSe_5 measured with both field-cooled (FC) and zero-field-cooled (ZFC) processes. The superconducting transition is observed at about 2.6 K. (b) Temperature dependence of the resistivity $\rho(T)$. The inset shows the superconducting transition at low temperature, with different definitions of the transition temperature T_c.

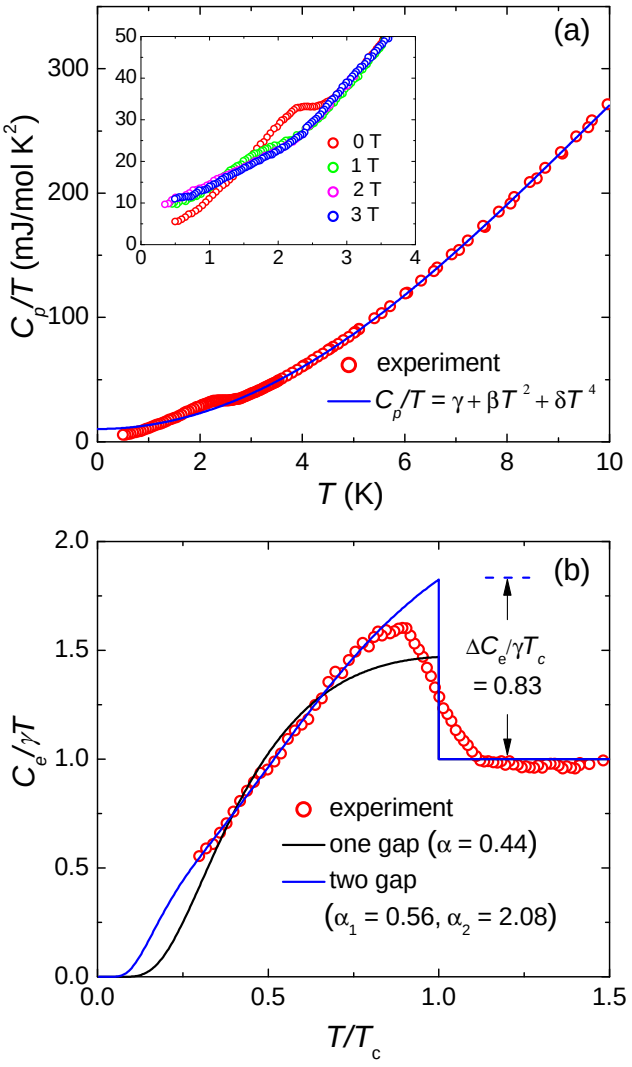

Fig. 3: (Color online) (a) Temperature dependence of specific heat divided by temperature C_p/T in zero field. The blue line is a fit to equation $C_p/T = \gamma + \beta T^2 + \delta T^4$. Inset: temperature dependence of C_p/T near the superconducting transition, measured at $H = 0$, 1, 2, and 3 T. (b) Reduced temperature T/T_c dependence of electronic specific heat divided by temperature C_e/T.

ing gap, we fit C_e/T in the superconducting state with the BCS α-model $C_e = C_0\exp(-\Delta/k_BT)$, where Δ is the size of the superconducting gap. It is found that the one-gap model with $\alpha \equiv \Delta/k_BT_c = 0.44$ can not describe the experimental data well, while the two-gap model with $\alpha_1 = 0.56$ and $\alpha_2 = 2.08$ gives the best fit [15]. The superconducting gap ratio $\Delta_l/\Delta_s \simeq 3.7$ is obtained. This result is consistent with the band structure calculation of T_2PdCh_5 [6,8,14]. Taking spin-orbit coupling into account, the calculated Fermi surface of Ta_2PdS_5 consists of a large hole sheet and two electron sheets (a large two dimensional cylinder around the zone center and small closed sections on the zone faces), and the superconductivity is likely to be dominated by the two larger sheets [14].

To estimate the coupling strength of Ta_2PdSe_5, the normalized specific heat jump $\Delta C_e/\gamma T_c$ is estimated to be about 0.83. This value is smaller than that expected for weak-coupling BCS superconductors ($\Delta C_e/\gamma T_c = 1.43$), which could be attributed to weak coupling strength or a sizeable nonsuperconducting fraction in Ta_2PdSe_5. Note that similar value $\Delta C_e/\gamma T_c = 0.9$ was also reported on the sister compound Nb_2PdS_5 [12,16].

Figure 4(a) shows the low-temperature resistivity of Ta_2PdSe_5 in various magnetic fields up to 14 T. As the magnetic field increases, T_c decreases and the superconducting transition broadens. At $H = 3$ T, the zero-resistivity superconductivity has already been suppressed below 0.3 K. The upper critical field $H_{c2}(T)$ versus reduced temperature T/T_c is shown in Fig. 4(b). The data points symbolled as H_{c2}^{onset} and H_{c2}^{mid} are extracted from each $\rho(T)$ curve in Fig. 4(a) according to the definitions of T_c^{onset} and T_c^{mid}. Both H_{c2}^{onset} and H_{c2}^{mid} increase with decreasing temperature, showing no sign of saturation at the lowest temperature, in contrast to that observed in a

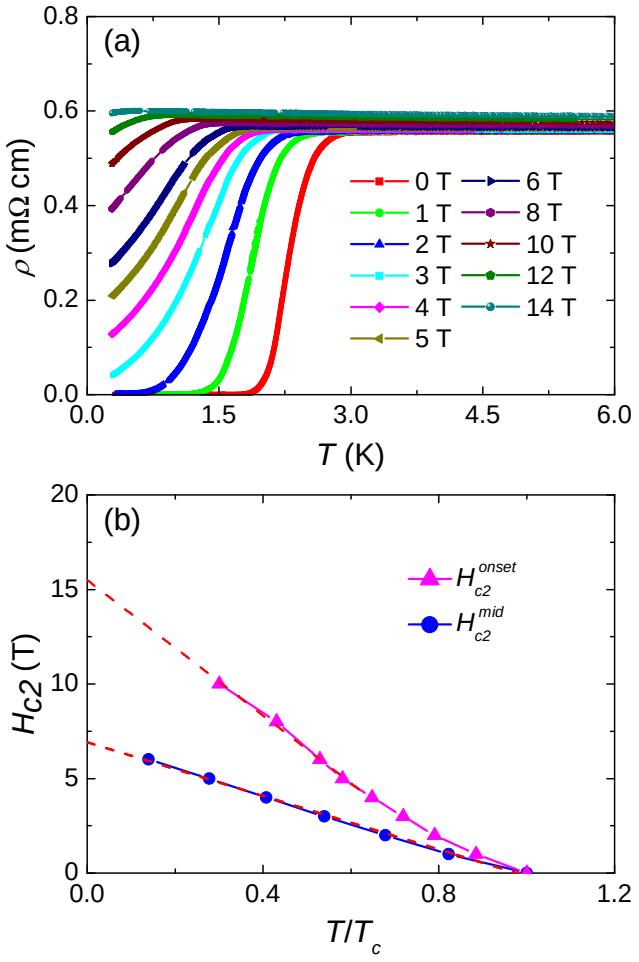

Fig. 4: (Color online) (a) Low-temperature resistivity $\rho(T)$ of Ta_2PdSe_5 in various magnetic fields up to 14 T. (b) Reduced temperature T/T_c dependence of the upper critical field $H_{c2}(T)$. The data points of H_{c2}^{onset} and H_{c2}^{mid} are extracted from each $\rho(T)$ curve in (a) according to the definitions of T_c^{onset} and T_c^{mid}.

conventional superconductor. More interestingly, the two curves show roughly linear temperature dependence at low temperature. We estimate $H_{c2}(0) \simeq 15.5$ T by linearly extrapolating the $H_{c2}^{onset}(T)$ curve to zero temperature. The corresponding ratio of $H_{c2}(0)/T_c$ comes out to be 6 T/K. In Table I, we list the T_c, γ, $H_{c2}(0)$, and $H_{c2}(0)/T_c$ for all four members of the T_2PdCh_5 family [6, 8, 9]. Both the linear temperature dependence of $H_{c2}(T)$ and the abnormally high $H_{c2}(0)/T_c$ are common features of T_2PdCh_5 [6, 8, 9].

In Fig. 4(b), a linear fit of the $H_{c2}^{onset}(T)$ data near T_c provides the initial slope $|dH_{c2}/dT_c|_{T_c} = 4.17$ T/K. For one-band BCS superconductors, orbital limiting field $H_{c2}^{orb}(0)$ is commonly derived from this slope, and Werthamer-Helfand-Hohenberg (WHH) theory predicts $H_{c2}^{orb}(0) = -0.69|dH_{c2}/dT_c|_{T_c}T_c$ in the dirty limit and $H_{c2}^{orb}(0) = -0.73|dH_{c2}/dT_c|_{T_c}T_c$ in the clean limit. For Ta_2PdSe_5, the Ginzburg-Landau coherence length $\xi_0 =$ 65.8 Å is calculated by using $\xi_0 = [\Phi_0/2\pi H_{c2}(0)]^{1/2}$. The electron mean free path $l \simeq 24$ Å is roughly estimated from ρ_0 and γ [8]. Since $l < \xi_0$, Ta_2PdSe_5 is close to dirty limit. Therefore, the orbital limit based on one-band WHH formula gives $H_{c2}^{orb}(0) = -0.69|dH_{c2}/dT_c|_{T_c}T_c = 7.28$ T. This value is higher than the expected weak coupling Pauli limiting field $H_{c2}^{P}(0) = 1.84T_c = 4.6$ T in the case of spin-singlet pairing, but still far below the measured $H_{c2}(0)$ value. Such an abnormal $H_{c2}(0)$ can not be understood in terms of one-band Ginsburg-Landau theory.

Table 1: Comparison among four T_2PdCh_5 (T = Nb or Ta, Ch = S or Se) compounds, including transition temperature T_c, electronic specific heat coefficient γ, upper critical field $H_{c2}(0)$ and the $H_{c2}(0)/T_c$ ratio. These values are taken from Refs. [6, 8, 9], and this work.

	T_c (K)	γ (mJ/mol K^2)	$H_{c2}(0)$ (T)	$H_{c2}(0)/T_c$ (T/K)
$Nb_2Pd_xS_5$	6.6	15	37	5.6
$Nb_2Pd_xSe_5$	5.0	12.8	35	5.9
$Ta_2Pd_xS_5$	5.4	27.6	31	5.7
Ta_2PdSe_5	2.5	10.3	15.5	6.2

The linear temperature dependence of $H_{c2}(T)$ was previously observed in two-band superconductor MgB_2 [17–19], and it was explained by Gurevich based on the dirty two-gap Usadel equations [20, 21]. Unlike one-gap theory in which $H_{c2}(T)$ has a downward curvature, $H_{c2}(T)$ of a dirty two-gap superconductor can show linear dependence or even upward curvature, depending on the intraband diffusion ratio caused by strong impurity scattering [20, 21]. Moreover, the interband scattering can make the $H_{c2}(0)$ significantly higher than that estimated from one-gap theory [22]. Therefore, we ascribe the linear temperature dependence of $H_{c2}(T)$ and the abnormally high $H_{c2}(0)/T_c$ observed in T_2PdCh_5 family to the multi-band effect. However, one may not ignore the effect of spin-orbital coupling, since large spin-orbit scattering due to Pd deficiency in these compounds can suppress the paramagnetic pair breaking, thus enhance the limit of the upper critical field [9]. From the perspective of application, Ta_2PdSe_5 and the related chalcogenides provide a new family of materials exhibiting high H_{c2}, which makes them candidate materials for high-field applications.

Summary. – In summary, a new transition-metal chalcogenide compound Ta_2PdSe_5 was first synthesized. Measurements of resistivity, magnetization and specific heat revealed that Ta_2PdSe_5 is a superconducting material with $T_c \simeq 2.5$ K. This compound displays a remarkably high upper critical field $H_{c2}(0)$ relative to its superconducting transition temperature T_c. Both the fit of electronic specific heat and the linear temperature dependence of H_{c2} indicate multi-band superconductivity in Ta_2PdSe_5.

Note added: Stimulated by the preprint of this work (arXiv:1412.6983), the electronic structure and related properties of Ta_2PdSe_5 were theoretically obtained from density functional calculations [23]. The Fermi surface has two disconnected sheets [23], which are consistent with our experimental results.

* * *

This work is supported by the Natural Science Foundation of China, the Ministry of Science and Technology of China (National Basic Research Program No: 2012CB821402 and 2015CB921401), China Postdoctoral Science Foundation No: 2014M560288, Program for Professor of Special Appointment (Eastern Scholar) at Shanghai Institutions of Higher Learning, and STCSM of China (No. 15XD1500200).

REFERENCES

[1] Matsuda Y. and Shimahara H., *J. Phys. Soc. Jpn.*, **76** (2007) 051005 .
[2] Clogston A. M., *Phys. Rev. Lett.*, **9** (1962) 266.
[3] Lee I. J., Chaikin P. M. and Naughton M. J., *Phys. Rev. B*, **62** (2000) R14669.
[4] Mercure J.-F., Bangura A. F., Xu Xiaofeng, Wakeham N., Carrington A., Walmsley P., Greenblatt M. and Hussey N. E., *Phys. Rev. Lett.*, **108** (2012) 187003.
[5] Lei H., Graf D., Hu R., Ryu H., Choi E. S., Tozer S. W. and Petrovic C., *Phys. Rev. B*, **85** (2012) 094515.
[6] Zhang Q., Li G., Rhodes D., Kiswandhi A., Besara T., Zeng B., Sun J., Siegrist T., Johannes M. D. and Balicas L., *Sci. Rep.*, **3** (2013) 1446.
[7] Squattrito P. J., Sunshine S. A. and Ibers J. A., *J. Solid State Chem.*, **64** (1986) 261.
[8] Khim Seunghyun, Lee Bumsung, Choi Ki-Young, Jeon Byung-Gu, Jang Dong Hyun, Patil Deepak, Patil Seema, Kim Rokyeon, Choi Eun Sang, Lee Seongsu, Yu Jaejun and Kim Kee Hoon, *New J. Phys.*, **15** (2013) 123031.
[9] Lu Yangfan, Takayama Tomohiro, Bangura Alimamy F., Katsura Yukari, Hashizume Daisuke and Takagi Hidenori, *J. Phys. Soc. Jpn.*, **83** (2014) 023702.
[10] Yu Hongyan, Zuo Ming, Zhang Lei, Tan Shun, Zhang Changjin and Zhang Yuheng, *J. Am. Chem. Soc.*, **135** (2013) 12987.
[11] Jha Rajveer, Tiwari Brajesh, Rani Poonam, Kishan Hari and Awana V. P. S., *J. Appl. Phys.*, **115** (2014) 213903.
[12] Niu C. Q., Yang J. H., Li Y. K., Chen Bin, Zhou N., Chen J., Jiang L. L., Chen B., Yang X. X., Cao Chao, Dai Jianhui and Xu Xiaofeng, *Phys. Rev. B*, **88** (2013) 104507.
[13] Zhou N., Xu Xiaofeng, Wang J. R., Yang J. H., Li Y. K., Guo Y., Yang W. Z., Niu C. Q., Chen Bin, Cao Chao and Dai Jianhui, *Phys. Rev. B*, **90** (2014) 094520.
[14] Singh David J., *Phys. Rev. B*, **88** (2013) 174508.
[15] Padamsee H., *J. Low Temp. Phys.*, **12** (1973) 387.
[16] Goyal Reena, Tiwari Brajesh, Jha Rajveer and Awana V. P. S., *arXiv:1412.4890*, (2014) .
[17] Buzea Cristina and Yamashita Tsutomu, *Supercond. Sci. Technol.*, **14** (2001) R115.
[18] Gurevich A, Patnaik S, Braccini V, Kim K H, Mielke C, Song X, Cooley L D, Bu S D, Kim D M, Choi J H, Belenky L J, Giencke J, Lee M K, Tian W, Pan X Q, Siri A, Hellstrom E E, Eom C B and Larbalestier D C, *Supercond. Sci. Technol.*, **17** (2004) 278.
[19] Ferrando V., Bernini C., Manfrinetti P., Marr D., Putti M., Tarantini C. and Ferdeghini C., *Physica C*, **408** (2004) 127.
[20] Gurevich A., *Phys. Rev. B*, **67** (2003) 184515.
[21] Gurevich A., *Physica C*, **456** (2007) 160.
[22] Mansor M. and Carbotte J. P., *Phys. Rev. B.*, **72** (2005) 024538.
[23] Singh David J., *arXiv:1504.01333*, (2015) .